Experimental Investigation of Mixing Phenomena in a Gas Stirred Liquid Bath

G. G. KRISHNA MURTHY, S. P. MEHROTRA, and A. GHOSH

Mixing phenomena in a room temperature water bath, agitated by injecting air through a straight circular nozzle fitted axially at the bottom of the vessel, were characterized by experimentally measuring mixing time (t_{mix}) by electrical conductivity technique. It was found that t_{mix} defined at 99.5 pct homogenization did not depend on location and size of conductivity probe, location of tracer injection, and the amount of tracer injected. t_{mix} decreased with increasing gas flow rate and bath height, but decreasing nozzle diameter. Visual observations of the two-phase plume and flow conditions in the bath revealed that the plume swirled above a certain gas flow rate which enhanced the mixing rates in the bath. The transitions in ln t_{mix} *vs* ln $\dot{\varepsilon}_b$ curves were found to correspond to onset of swirling; $\dot{\varepsilon}_b$ is the rate of buoyancy energy input per unit bath volume. Systematic analysis of experimental data revealed that a fraction of gas kinetic energy contributed to mixing in the bath. It was a function of bath height, being negligible at lower bath heights and almost 1 at larger bath heights. Further, it was experimentally found that t_{mix} decreased with increasing bath height only up to a certain value, beyond which it started increasing. Visual observations of the bath revealed that the height at which t_{mix} started increasing corresponded to a transition in which the bath was converted into a bubble column. The experimental data, for a particular bath height, were fitted into two separate straight lines of the form $t_{mix} = c\dot{\varepsilon}^{-n}$, where c and n are empirical constants and $\dot{\varepsilon}$ is the rate of energy input per unit bath volume.

I. INTRODUCTION

INHOMOGENEITIES in concentration as well as temperature are reduced by the mixing operation in the process industry. In high temperature metallurgical melts mixing is often carried out by injection of a gas either from the top or bottom of the vessel. It is generally believed that the mixing is more effective when the gas is injected from the bottom. There are many metallurgical processes, *e.g.*, ladle treatment of liquid metals, oxygen steelmaking processes, *etc.*, in which mixing is promoted by injecting/purging gases from the bottom of the vessel.[1–6] When a gas is injected into a liquid bath from the bottom at a moderate flow rate it comes out of the nozzle in the form of gas bubbles. These gas bubbles rise to the bath surface due to buoyancy effect and impart momentum to the surrounding liquid, causing gross circulation in the bath and thereby promoting mixing.

Generally speaking, the purpose of stirring is to supply the system with energy which results in the circulation of the liquid and hence mixing in the bath. Inefficient stirring leads to higher power consumption which, in turn, adversely affects the process economy. Therefore, a vital issue in the processes involving liquids is the relationship between mixing and the nature of fluid flow. A detailed knowledge of hydrodynamics in the vessel will be useful in analyzing the process performance. However, such knowledge is very difficult to attain in view of the presence of complex time-dependent three-dimensional turbulent flow. Experimental measurements of velocity distribution is an obvious answer, but it is fairly complex. Fortunately, an alternative can be found in which some gross integral quantities are more easily determined. One of these is 'mixing time', which is frequently employed to characterize the mixing phenomena in liquid baths. Mixing time (t_{mix}) is defined as the time required to attain desired level of homogeneity in the bath (or desired value of degree of mixing (Y)).[7]

Direct measurement of t_{mix} in high temperature melts, although desirable, is expensive and difficult. To overcome this problem, cold model studies involving water as experimental fluid and glass or plexiglass vessel as reactor vessel are often carried out. One of the most commonly used techniques of experimentally measuring t_{mix} is based on what is known as 'stimulus response technique'. Based on this technique, various methods of measuring t_{mix} in liquid baths at room temperature have been developed. These include colored dye technique,[8,9] decolorization technique,[10–14] measurement of temperature profiles using thermocouples,[10,15,16] pH measurement,[17,18] refractive index measurement,[19] and electrical conductivity measurement.[20–27] Merits and demerits of these various methods have been discussed in detail elsewhere.[28]

In gas stirred liquid baths t_{mix} is expected to depend on gas flow rate, bath height and diameter, and nozzle diameter. In addition, vessel shape, nozzle position in the bottom of the vessel, number of nozzles used, and physical properties of liquid will also influence t_{mix}. However, the present study is confined to single nozzle placed axially at the bottom of a cylindrical vessel.

Although there are many reported studies in the literature[12,17,25,26,29–31] on the effects of gas flow rate, bath height, and bath diameter on mixing time in water and molten metal baths, little is reported about the effect of gas-nozzle diameter. Even the investigations on the reported variables

G. G. KRISHNA MURTHY, formerly Graduate Student in the Department of Metallurgical Engineering at the Indian Institute of Technology, Kanpur, India, is Postdoctoral Fellow, Department of Materials Science and Engineering, Massachusetts Institute of Technology, Cambridge, MA 02139. S. P. MEHROTRA and A. GHOSH are Professors, Department of Metallurgical Engineering, Indian Institute of Technology, Kanpur 208016, India.

Manuscript submitted February 9, 1987.

are far from extensive and there are many unexplained phenomena. In the present investigation, the mixing phenomena in gas stirred water bath at room temperature have been studied and an attempt is made to resolve some of the existing inconsistencies. The mixing time has been experimentally determined using the electrical conductivity method at various gas flow rates, bath heights, and nozzle diameters. Experimental results have been discussed in terms of mixing energy and the role of gas kinetic energy recognized.

II. EXPERIMENTAL

A. *Experimental Set-up*

The experimental set-up employed a cylindrical plexiglass vessel containing distilled water at room temperature. The water bath was stirred by injecting air through a straight circular nozzle fitted axially at the bottom of the vessel. Schematic representation of the experimental set-up is shown in Figure 1. It was fabricated and used earlier for shear stress measurements by Ballal and Ghosh and described in detail elsewhere.[32] The vessel used in the present investigation consisted of a tank of 0.51 m × 0.51 m square cross-section and 0.67 m height made of 10 mm thick, optically clear, plexiglass sheet. A cylindrical plexiglass vessel of 0.48 m i.d. and 0.65 m height, open at both ends, was placed inside the square vessel. The annular space between the two tanks was filled with water during the experiments to avoid optical distortions. The lower end of the cylindrical vessel was sealed against the bottom of the square vessel by a neoprene gasket, applying pressure from the top. The bottom of the vessel had a centrally threaded hole into which the nozzle could be fitted. A few experiments, however, were also carried out in a cylindrical glass vessel of 0.125 m i.d. and 1.10 m length. This vessel, which was mainly used for measurements at higher H/D ratios, was also enclosed in the square tank.

Gas nozzles were in the form of straight circular pipes. Experiments were carried out using nozzles of four different sizes (2.77 mm, 3.87 mm, 6.66 mm, and 10.0 mm) with 0.48 m i.d. vessel, and a nozzle of 1.60 mm i.d. with 0.125 m i.d. vessel. Only one nozzle was used at a time.

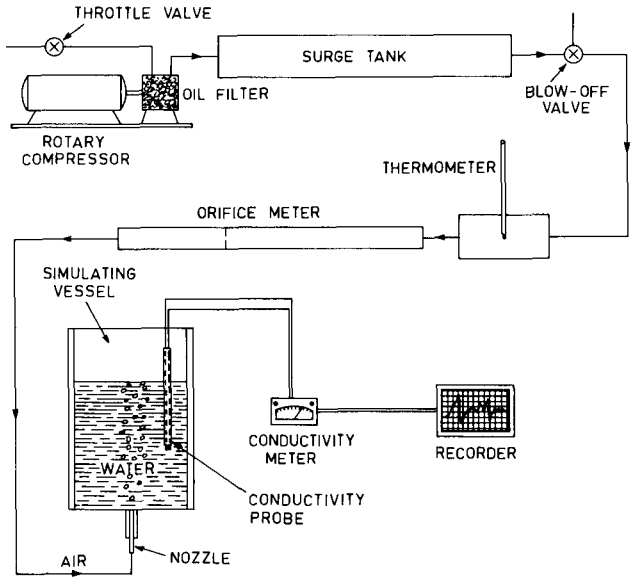

Fig. 1—Schematic representation of experimental set-up.

Air was supplied by a 3 H.P. rotary compressor-cum-blower pump. Air flow rates in the range 2.2×10^{-4} to 36.0×10^{-4} Nm^3/s were measured with an orifice meter, which had been fabricated to ASME specifications,[33] while a wet test meter was employed to measure the air flow rates up to 2.2×10^{-4} Nm^3/s. Using the standard method of error analysis, the maximum error in measured air flow rate was estimated to be around 6 pct.

B. *Mixing Time Measuring Technique*

Of the various methods reported in literature for the mixing time measurements, methods based on pH and electrical conductivity measurements are perhaps most convenient. In these methods a tracer in the form of an acid, alkali, or a salt solution is injected as an impulse and variation in pH/electrical conductivity as a function of time recorded. However, the pH measurement suffers from the following limitations:

(i) pH probe is fragile and therefore difficult to handle, and (ii) pH of the bath is proportional to the logarithm of the tracer concentration which shows less sensitivity to concentration variations during mixing.

The electrical conductivity probe (henceforth to be called ECP), on the other hand, is sturdy and has a faster response. Moreover, electrical conductivity varies linearly with the tracer concentration in the range of present measurements. Further, it can be used for a wide range of homogenization measurements, and estimation of precise value of mixing is easier.[34,35] Hence, ECP was preferred over pH probe and was employed in the present investigation.

Schematic representation of the ECP, designed and fabricated to measure the variations of KCl concentration in the distilled water bath when the former is added in small quantities as a tracer, is shown in Figure 2(a). The probe employed in most of the measurements consisted of two thin parallel platinum foils of approximately 10 mm × 10 mm square cross-section placed 3.2 mm apart. The distance between the two electrodes was purposely kept small to allow only a small volume of liquid to be entrained between the electrodes. The electrode foils were backed by 2.0 mm thick perspex pieces, rigidly fixed in order to avoid any vibrations coming from the turbulence in the bath. The electrode assembly was encased in a grounded copper tube to minimize extraneous disturbances due to the impact of the liquid flow as well as outside electrical fields.

The electrical circuit employed is shown in Figure 2(b). It involved the probe and an electrical conductivity meter which had an in-built 1 kHz signal generator. Since the conductivity meter worked as an unbalanced Wheatstone bridge, the unbalanced voltage was related to the resistance of the ECP which was inversely proportional to specific conductance of the electrolyte. The latter was, in turn, proportional to the concentration of the tracer at the point of measurement. Therefore, this unbalanced voltage was measured as a function of time, employing a dual pen strip chart recorder.

C. *Experimental Procedure*

Before starting any measurements, air was blown into the distilled water bath at a specified flow rate for 10 to

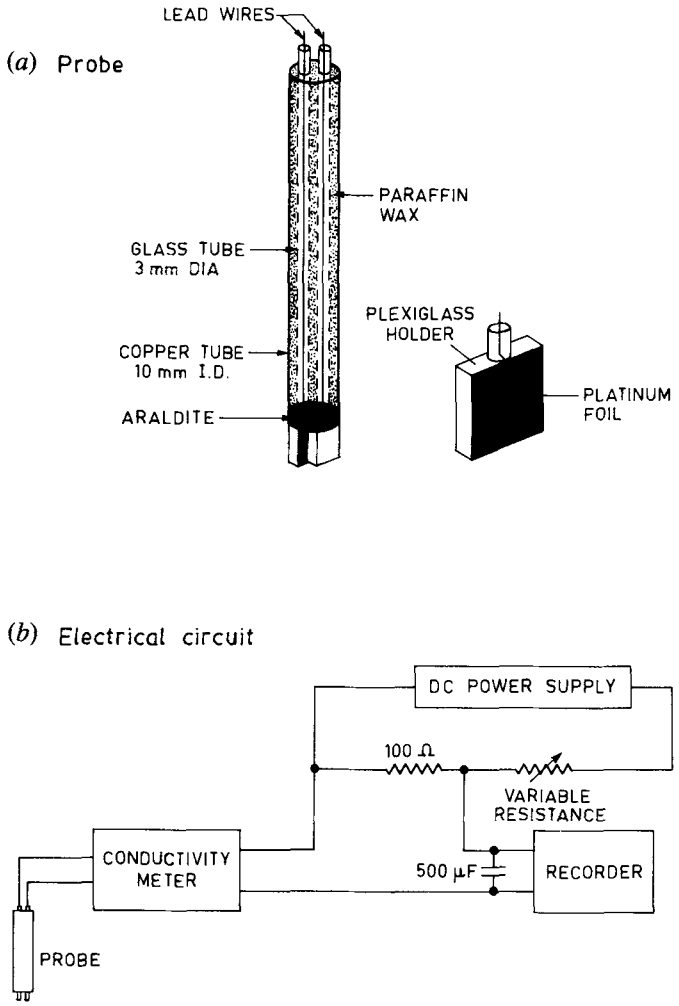

Fig. 2—(*a*) Electrical conductivity probe and (*b*) electrical circuit used for mixing time measurements.

15 minutes to ensure the stability of the flow in the vessel as well as to homogenize the initial bath composition. A small amount of KCl solution was injected as tracer onto the bath surface. The voltage-time traces obtained on the recorder chart (Figure 3) were analyzed for t_{mix} estimation.

On addition of tracer, considerable oscillations in the form of peaks and valleys were observed on the chart. These peaks and valleys result from the concentration fluctuations at the probe tip arising from inhomogeneities of tracer concentration in the bath. The fluctuations gradually decay and attain a steady value which is reflected in an almost steady voltage on the chart. Experimentally determined t_{mix} is the time required for the voltage to reach this steady fluctuation range.[35,36] Detailed discussion on determination of this steady voltage range and its relationship to the 'degree of homogenization' has been presented in one of our earlier papers.[36]

III. RESULTS

To check the reproducibility of the measurements, they were repeated several times (sometimes more than 100 times) under identical conditions and t_{mix} was determined. It was found that the variation in t_{mix} between run to run was within

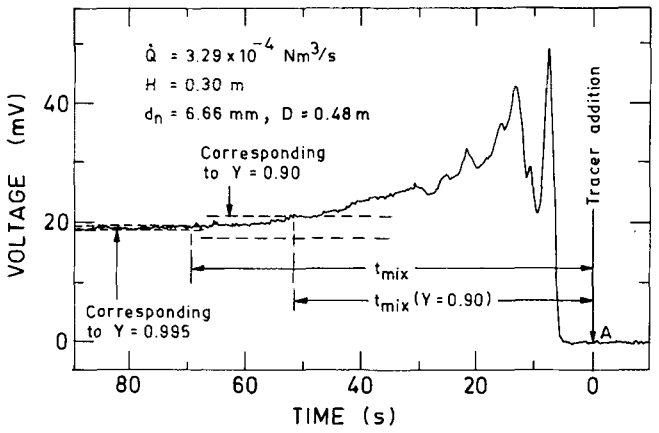

Fig. 3—A typical recorder voltage-time trace showing mixing time at two different values of degree of mixing.

±5 pct at higher values of t_{mix} and ±10 pct at lower values of t_{mix}. Further, in order to check that the measured t_{mix} can be employed as a parameter characterizing the mixing in the entire bath and that it is not a property in a localized zone in the vicinity of the probe electrodes, it was necessary to examine the influence of probe location, probe size, location of tracer injection point, and amount of tracer injected on t_{mix}. These results have been presented elsewhere.[35,36]

To sum up, it was established that the measured t_{mix} was indeed independent of all these parameters. In the present investigation, probes of three different sizes (5 mm × 5 mm, 10 mm × 10 mm, and 20 mm × 20 mm) were used to study probe size effect on t_{mix}. The size of each probe was larger than the smallest eddy size which is less than 100 μm. Therefore, in this investigation only macromixing was examined and the probe size did not affect the measurements. Hence, t_{mix} though measured with the probe at a certain fixed location in the bath, could be employed as a parameter to characterize the mixing phenomena in the entire bath.

As it is obvious from the definition of mixing time, the experimentally measured t_{mix} depends on the degree of mixing (Y).[36,37] It must be emphasized that the comparison of experimentally determined values of t_{mix} will be meaningful only when they are measured at the same value of Y. In the present study, all measurements were made at $Y = 0.995$.

The ranges of various operating variables at which t_{mix} was measured are presented in Table I. In all, about 4000 measurements were made. Some typical values of t_{mix} for various experimental conditions are presented in Table II. Each value represents the average of 8 or more experimental runs. Some typical plots showing the variation of t_{mix} with operating variables are presented in Figures 4 to 6. These results are discussed in detail in the following section.

IV. DISCUSSION

A. *Influence of Gas Flow Rate on Mixing*

Figure 4 shows the variation of t_{mix} with gas flow rate ($\dot{Q}$). t_{mix} decreases with increasing Q. This observation is in agreement with those reported in literature.[12,17,25,26,29] Guthrie[29] found t_{mix} to be proportional to $\dot{Q}^{-1/3}$. When a gas is injected into a liquid bath through a nozzle fitted at the bottom of the vessel, it provides energy required for the mix-

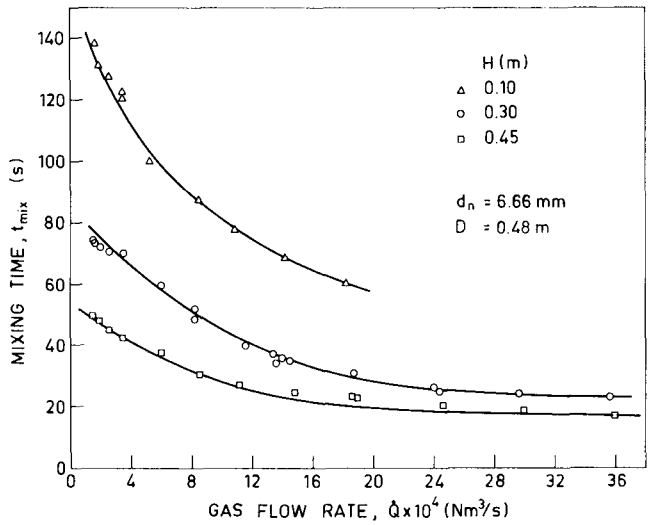

Fig. 4—Effect of gas flow rate on mixing time at three different bath heights.

Table I. Operating Variables and Their Ranges Employed in the Measurements of Mixing Time in the Vessel of 0.48 m Diameter and 0.65 m Height

Variable	Range
Gas flow rate, $\dot{Q} \times 10^4$ (Nm³/s)	1.50 to 36.0
Bath height, H (m)	0.10, 0.15, 0.20, 0.25, 0.30, 0.35, 0.40, 0.45
Nozzle diameter, d_n (mm)	2.77, 3.87, 6.66, 10.00

ing of the bath. It is, therefore, only proper to express the mixing rates as a function of some appropriate energy term.

The energy term that is normally used for this purpose is the rate of energy dissipation per unit volume of liquid ($\dot{\varepsilon}$). Truly speaking, it is a function of both the rate of input of kinetic energy of gas per unit volume of liquid ($\dot{\varepsilon}_k$) and the rate of buoyancy energy input per unit volume of liquid ($\dot{\varepsilon}_b$).

Neglecting the work done by the expanding gas bubbles at the nozzle exit due to the change in pressure and temperature, Bhavaraju *et al.*[38] derived the following equation correlating the rate of buoyancy energy per unit volume of liquid to other variables:

$$\dot{\varepsilon}_b = \frac{4\dot{Q}P_{atm}T_L}{298.2\pi D^2 H} \ln\left(1 + \frac{\rho_L g H}{P_{atm}}\right) \qquad [1]$$

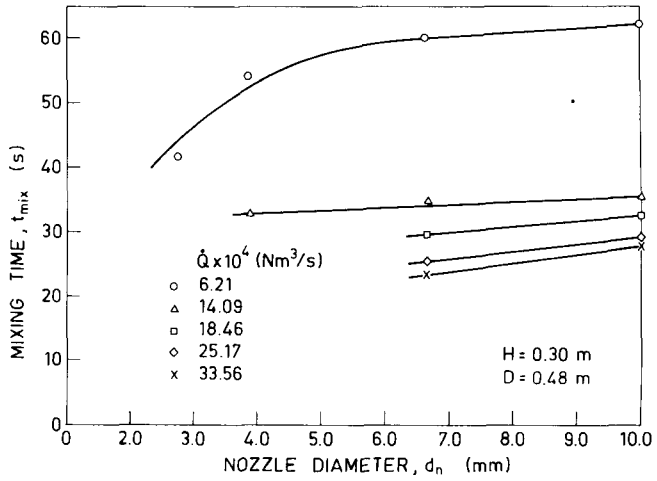

Fig. 5—Effect of nozzle diameter on mixing time at five different gas flow rates.

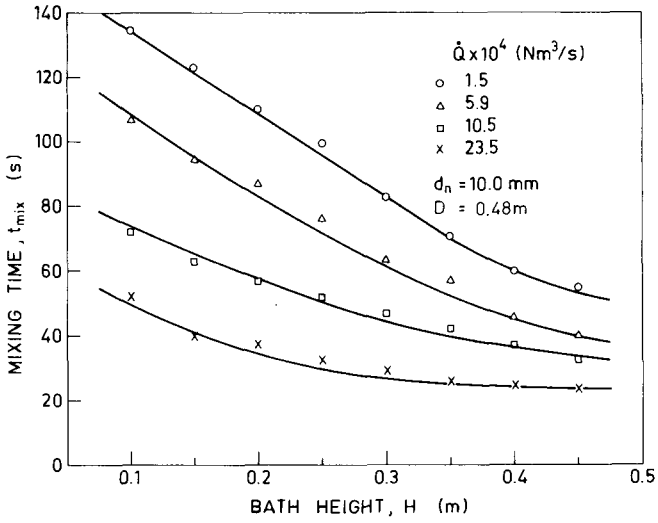

Fig. 6—Effect of bath height on mixing time at four different gas flow rates.

where $\dot{Q}$ is gas flow rate at NTP, D and H are bath diameter and height, respectively, ρ_L is liquid density, T_L is liquid temperature, g is acceleration due to gravity, and P_{atm} is atmospheric pressure. The kinetic energy of gas may be expressed as

$$\dot{\varepsilon}_k = \frac{32\rho_G \dot{Q}^3}{\pi^3 d_n^4 D^2 H} \qquad [2]$$

where ρ_G is density of gas and d_n is nozzle diameter.

Table II. Experimentally Determined t_{mix} as a Function of Operating Variables

$\dot{Q} \times 10^4$ (Nm³/s)	t_{mix} (s)							
	d_n (mm) = 10.00				6.66			
	H (m) = 0.10	0.20	0.30	0.40	0.10	0.20	0.30	0.40
1.49	133.8	109.9	82.6	59.6	137.9	93.1	74.3	55.2
5.86	106.5	87.5	62.4	44.6	—	84.4	59.7	40.5
10.45	76.0	57.8	47.6	37.5	77.6	61.8	43.7	34.7
18.32	52.6	40.3	32.8	27.6	60.4	42.6	29.9	25.4
24.34	—	—	29.4	24.8	—	—	25.5	23.1
29.41	—	—	28.9	22.8	—	—	24.0	21.9

Neglecting the contribution of $\dot{\varepsilon}_k$ to total $\dot{\varepsilon}$, especially for subsonic gas velocities, most of the earlier investigators related t_{mix} to $\dot{\varepsilon}_b$ only. The variation of measured t_{mix} with $\dot{Q}$, therefore, has also been expressed in terms of $\dot{\varepsilon}_b$. Figures 7 to 10 show the variation of t_{mix} with $\dot{\varepsilon}_b$ for different bath heights and nozzles of four different diameters. In these plots the experimental data seem to fall on two distinct straight lines. While the experimental observations of Asai *et al.*[25] are in conformity with those in the present study, most other investigators reported a linear relationship between ln t_{mix} and ln $\dot{\varepsilon}_b$

$$\ln t_{mix} = a - n \ln \dot{\varepsilon}_b \qquad [3]$$

where a and n are empirical constants. It is to be noted that each of the two linear segments of a graph in Figures 7 to 10 has the similar mathematical form, but the values of parameters a and n are different.

It is apparent that the increased energy input to the bath would increase the turbulence as well as bulk velocity which, in turn, decrease t_{mix}. Thus, the values of n would always be positive. However, in Figures 7 to 10 values of n for linear segments corresponding to the lower range of $\dot{\varepsilon}_b$ are always less than those corresponding to the higher range of $\dot{\varepsilon}_b$. This is in contrast to the observations of Asai *et al.*,[25] who reported $n = 0.68$ in the lower ranges and $n = 0.32$ in higher ranges of $\dot{\varepsilon}_b$. The flow rates studied by them corresponded to much lower values of $\dot{\varepsilon}_b$ and they attributed the change in n value to laminar-turbulent transition. In the present study the flow was always in the turbulent range, but even then a transition in ln t_{mix} *vs* ln $\dot{\varepsilon}_b$ curves in Figures 7 to 10 is apparent. This transition is represented by the intersection of two straight lines. Various possible explanations for this behavior were considered, but it appeared that this transition was most likely due to the onset of swirling motion (rotation) of the plume. Some typical photographs in Figure 11 reveal this behavior. It was, therefore, decided to investigate this aspect further in detail.

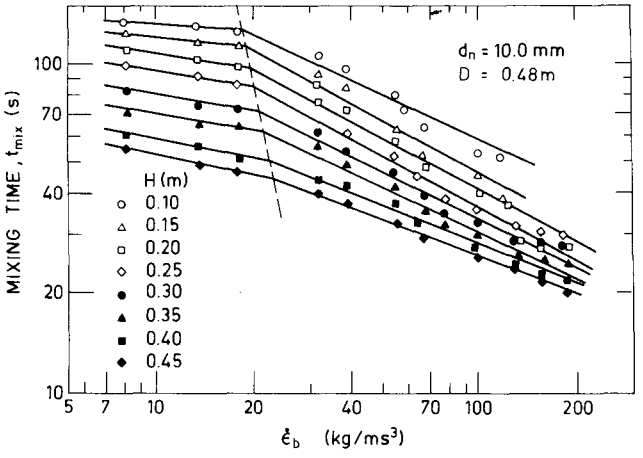

Fig. 7—Variation of mixing time with $\dot{\varepsilon}_b$ at eight different bath heights for a nozzle of 10.0 mm diameter.

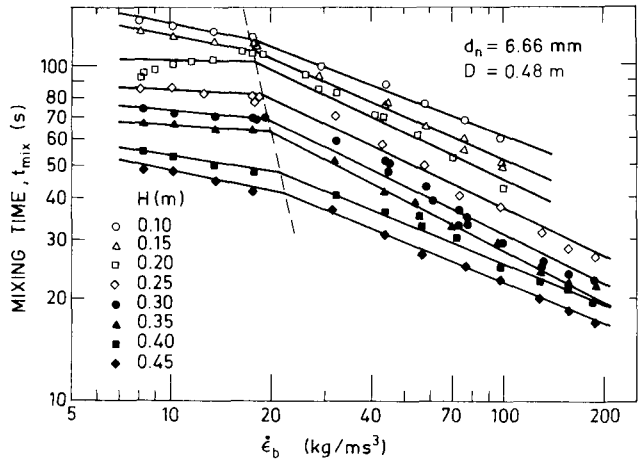

Fig. 8—Variation of mixing time with $\dot{\varepsilon}_b$ at eight different bath heights for a nozzle of 6.66 mm diameter.

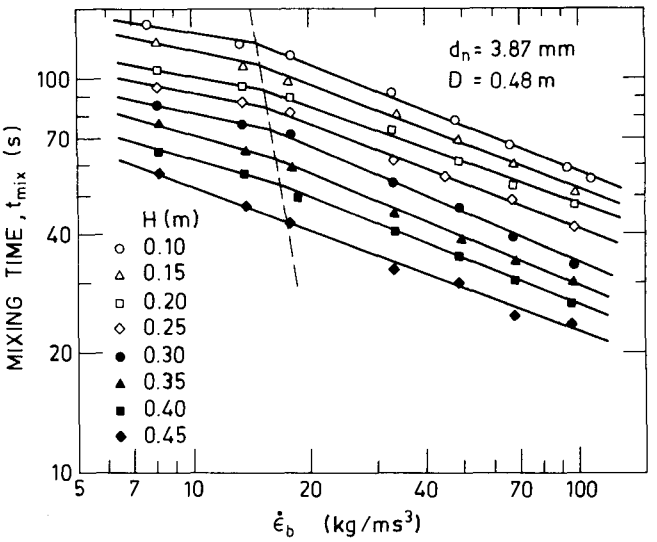

Fig. 9—Variation of mixing time with $\dot{\varepsilon}_b$ at eight different bath heights for a nozzle of 3.87 mm diameter.

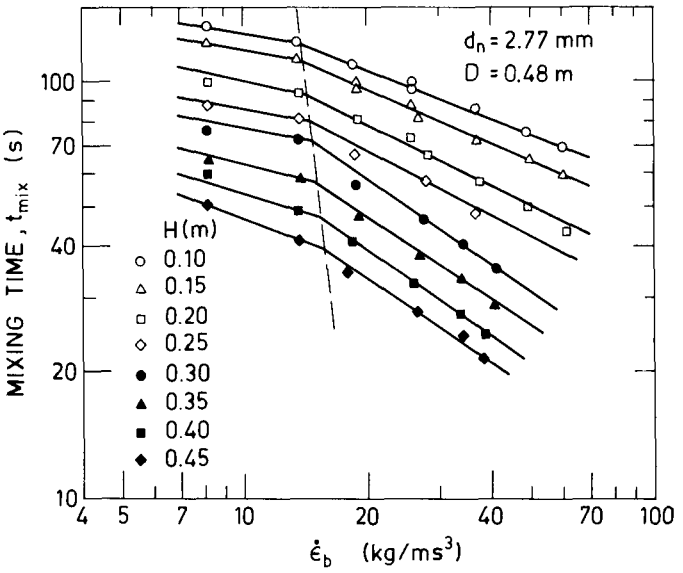

Fig. 10—Variation of mixing time with $\dot{\varepsilon}_b$ at eight different bath heights for a nozzle of 2.77 mm diameter.

B. *Swirling Motion of the Plume*

As the gas flow rate increases, the spout of the plume at the bath surface becomes larger and larger. At a certain

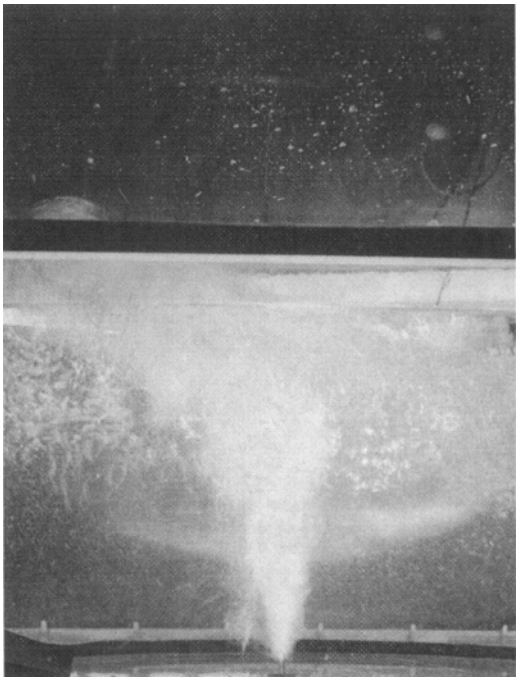

(*a*)

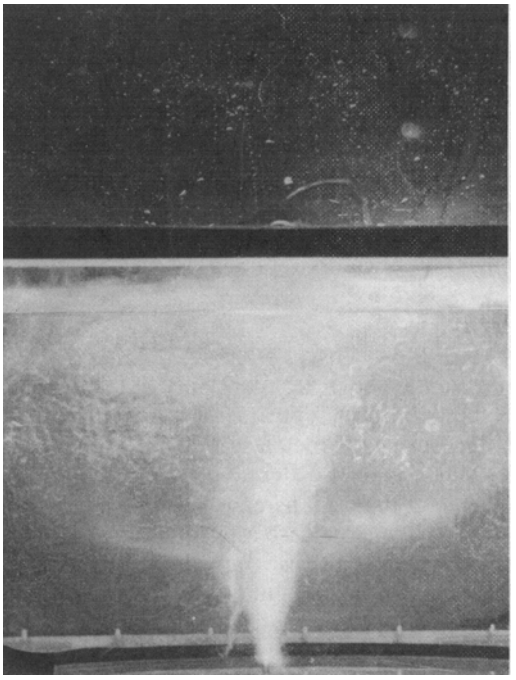

(*b*)

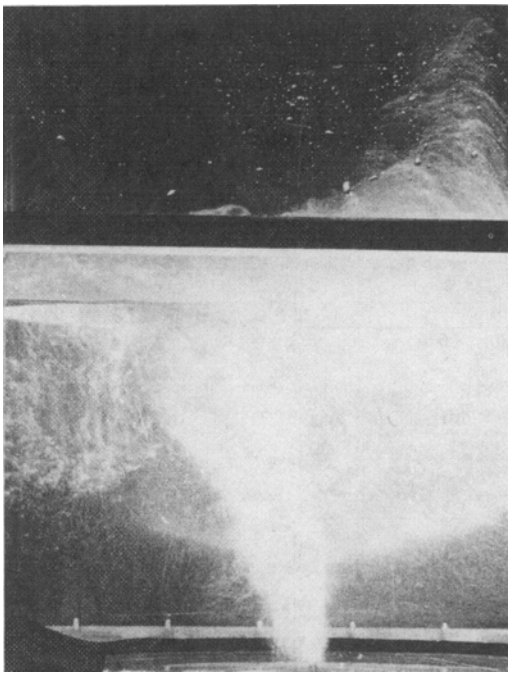

(*c*)

Fig. 11 — A set of still photographs showing the swirling of plume (H = 0.25 m, d_n = 3.87 mm, and $\dot{Q}$ = 17.5 × 10^{-4} Nm^3/s).

stage it starts oscillating, leading to vigorous wave motion at the bath surface which, in turn, causes the plume to rotate. For a systematic study of the onset of swirling motion, visual observations of the plume were made for gradually increasing gas flow rate starting with a very low value. At each value of $\dot{Q}$ sufficient time was allowed for the flow to stabilize. Onset of swirling motion of the plume, under various operating conditions, could be recorded by careful visual examination. Each observation was repeated at least three times.

The onset of the swirling motion of the plume at low bath heights was very clear and easy to record. With large bath heights, however, the observations were not so precise, and hence, instead of reporting a single value of $\dot{\varepsilon}_b$ at which swirling began, a range of $\dot{\varepsilon}_b$ has been noted. This value of $\dot{\varepsilon}_b$ at which swirling began is indicated by $\dot{\varepsilon}_{bs}$. Figure 12 shows the variation of $\dot{\varepsilon}_{bs}$ with bath height for nozzles of four different sizes. Since a range of $\dot{\varepsilon}_b$ values was assigned for $\dot{\varepsilon}_{bs}$, the variation of $\dot{\varepsilon}_{bs}$ with different operating conditions has been shown by the shaded areas in the figure. It may be noted that $\dot{\varepsilon}_{bs}$ increased with increasing both H and d_n.

The value of $\dot{\varepsilon}_b$ at transition in a ln t_{mix} *vs* ln $\dot{\varepsilon}_b$ curve (Figures 7 to 10) is designated by $\dot{\varepsilon}_{bc}$. The values of $\dot{\varepsilon}_{bc}$ read from these graphs are plotted along with $\dot{\varepsilon}_{bs}$ values in Figure 12. It is to be noted that for all experimental conditions, the values of $\dot{\varepsilon}_{bc}$ fell inside the shaded areas corresponding to $\dot{\varepsilon}_{bs}$. It is, therefore, concluded that the agreement between $\dot{\varepsilon}_{bs}$ and $\dot{\varepsilon}_{bc}$ (as in Figure 12) is quite good and that the intersection points in Figures 7 to 10 are indeed owing to the transition in flow pattern due to the onset of swirling motion of the plume.

In a set of experiments a short cylinder of 0.10 m diameter and 0.15 m length, open at both ends, was used as a spout breaker to reduce the swirling motion of the plume. The breaker was placed vertically, about 25 mm, above the quiescent bath surface and its interference with flow of liquid was kept to a minimum. This arrangement drastically cut down the amplitude of the oscillations of the bath surface. The variation of t_{mix} with $\dot{\varepsilon}_b$ in the experimental set-up with spout breaker is shown in Figure 13. It is evident that while the mixing time in the bath with spout breaker arrangement is larger than that for the bath without it for high values of $\dot{\varepsilon}_b$, it remained unchanged at low values where the swirling was anyway absent. Larger mixing time required for the bath with the spout breaker is, therefore, attributed to the reduced swirling motion of the plume. Visual examination of the plume in the presence of spout breaker clearly revealed that the plume began to swirl considerably only at higher values of $\dot{\varepsilon}_b$.

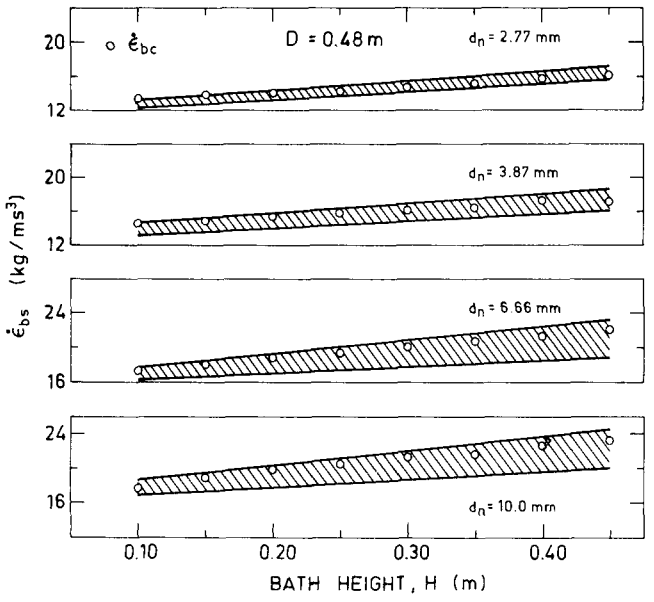

Fig. 12—Variations of $\dot{\varepsilon}_{bs}$ and $\dot{\varepsilon}_{bc}$ with bath height for nozzles of four different diameters.

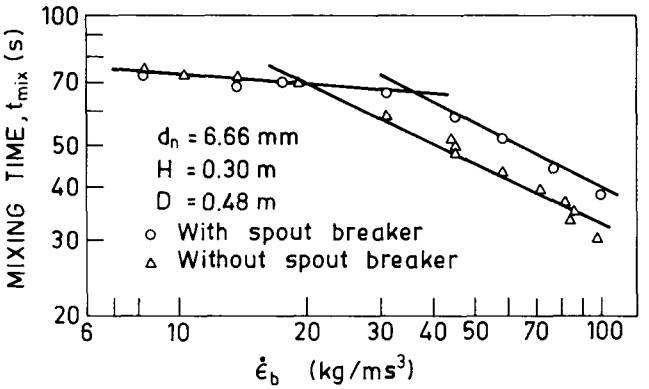

Fig. 13—Variation of mixing time with $\dot{\varepsilon}_b$ in the experimental set-up using spout breaker arrangement.

C. *Contribution of Kinetic Energy of Gas to Mixing*

Variation of t_{mix} with d_n at five different gas flow rates is presented in Figure 5. Mixing time increased with increasing nozzle diameter. This can be explained in terms of kinetic energy ($\dot{\varepsilon}_k$) contribution to mixing. In general, the total rate of energy dissipation per unit volume of liquid ($\dot{\varepsilon}$) in a mixing vessel can be taken as the sum of $\dot{\varepsilon}_b$ and a fraction of $\dot{\varepsilon}_k$, *i.e.*,

$$\dot{\varepsilon} = \dot{\varepsilon}_b + x\dot{\varepsilon}_k \qquad [4]$$

where x is the fraction of $\dot{\varepsilon}_k$ contributing to mixing and has a value between 0 and 1.

Assuming that the contribution of $\dot{\varepsilon}_k$ to mixing is negligible, most of the earlier investigators took the parameter x equal to zero.[30,38–40] Lehrer[22] suggested a value of 0.06 for x. In a recent study Haida and Brimacombe,[26] however, re-examined this aspect and arrived at the conclusion that about 15 pct of $\dot{\varepsilon}_k$ contributes to mixing. To resolve this controversy regarding the value of x, the role of gas kinetic energy in the mixing process has been examined in detail in the present study. The analysis and results are presented below.

From Eqs. [1] and [2], while $\dot{\varepsilon}_b$ is unaffected by both H and d_n (since $1/H$ ln$[1 + (\rho_L g H/P_{atm})] \simeq 0.10$), $\dot{\varepsilon}_k$ is a strong function of both of these ($\dot{\varepsilon}_k \propto H^{-1} d_n^{-4}$). Since $\dot{\varepsilon}_b$ is independent of nozzle diameter, the plots of ln t_{mix} *vs* ln $\dot{\varepsilon}_b$ for nozzles of different diameters should fall on a single curve, if no other effect of d_n on t_{mix} is expected. Figure 14 shows plots of ln t_{mix} *vs* ln $\dot{\varepsilon}_b$ for all nozzles at three different bath heights (0.10 m, 0.30 m, and 0.45 m). In the latter two cases scatter of the points is more than the expected experimental error in t_{mix} measurements, which indicated that d_n did affect t_{mix}, especially at larger bath heights. Values of $\dot{\varepsilon}_b$ and $\dot{\varepsilon}_k$ were computed for various values of $\dot{Q}$, H, and d_n, and are presented in the form of $\dot{\varepsilon}_k/\dot{\varepsilon}_b$ in Table III. It is apparent that the ratio $\dot{\varepsilon}_k/\dot{\varepsilon}_b$ is almost negligible for nozzles of larger diameters and smaller gas flow rates. However, the value becomes significant at higher gas flow rates, particularly with nozzles of smaller diameter.

If it is assumed that a fraction of $\dot{\varepsilon}_k$ contributes to mixing, t_{mix} should be a function of $\dot{\varepsilon}^{-n}$ and not $\dot{\varepsilon}_b^{-n}$. Only when $\dot{\varepsilon}_k$ contribution is negligible, Eq. [3] is valid. If, somehow, the right value of parameter, x, is known, $\dot{\varepsilon}$ can be evaluated using Eq. [4] and the plot of ln t_{mix} *vs* ln $\dot{\varepsilon}$ should be independent of d_n. This concept was utilized in estimating the value of x. The approach involved least square fitting of

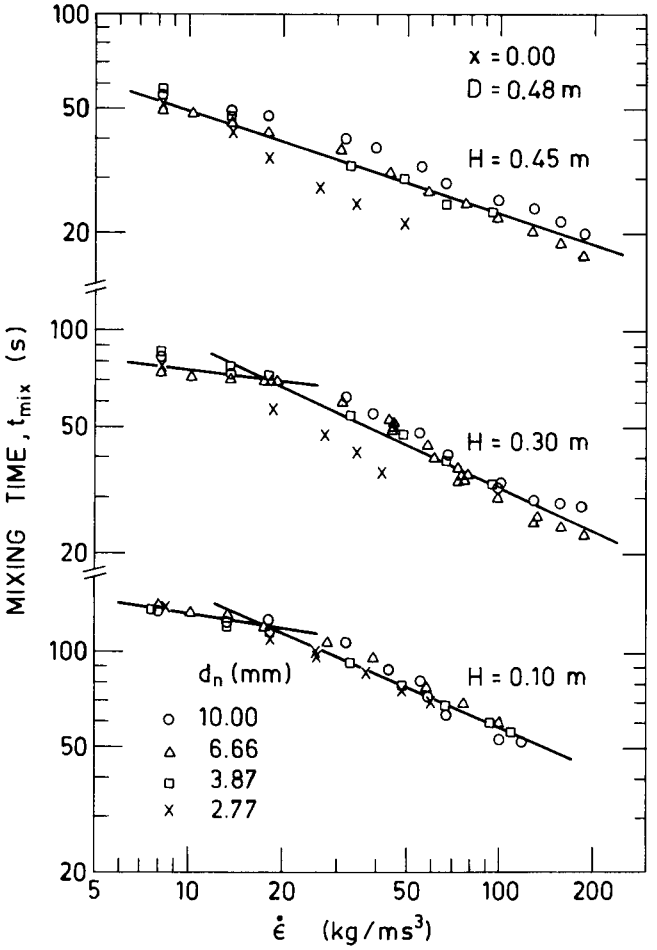

Fig. 14—Variation of mixing time with $\dot{\epsilon}(\dot{\epsilon}_b + x\dot{\epsilon}_k)$ at $x = 0$ for three different bath heights and for four different size nozzles.

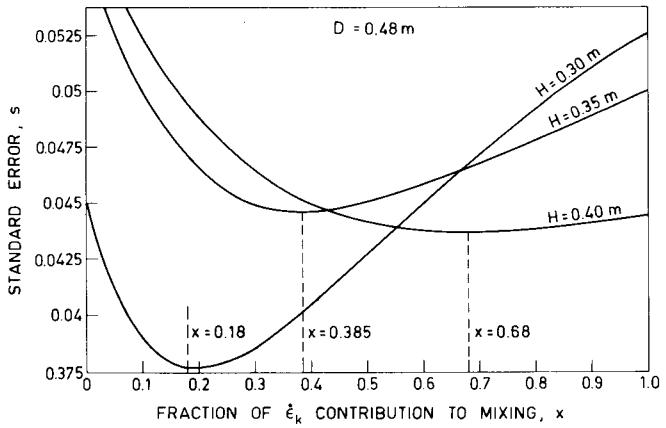

Fig. 15—Variation of standard error with fraction of gas kinetic energy contributing to mixing at three different bath heights.

the plotted points and estimating the standard error, s, for various values of x. Variation of s with x for three different bath heights is shown in Figure 15. The value of x, at which s was minimum, was taken as the appropriate one. Figure 16 shows the variation of x with H (and also with ratio H/D)—it increases with increasing H. This is also expected, for the larger the H, the more the gas has an oppor-

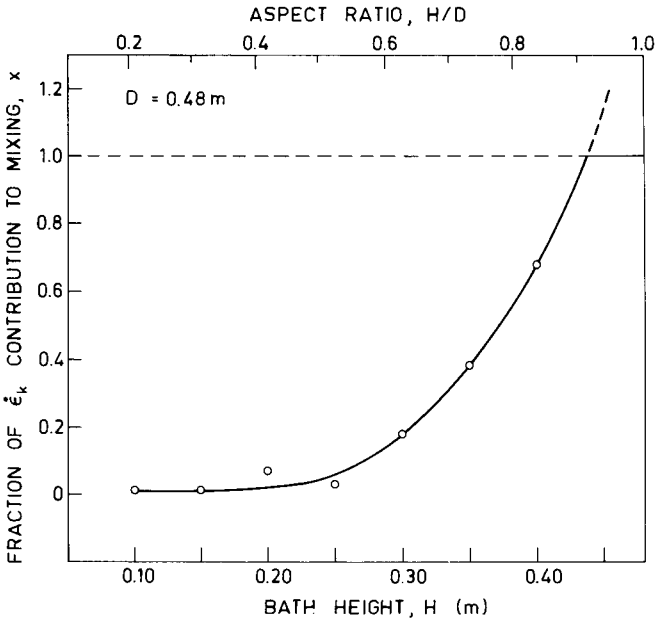

Fig. 16—Variation of fraction of gas kinetic energy contributing to mixing with bath height.

tunity to impart its kinetic energy to the liquid. In most of the investigations reported so far, the nozzle diameter has not been specified. This is perhaps one of the factors which is responsible for some confusion regarding the contribution of kinetic energy to mixing. As may be noted from Table III, the ratio $\dot{\epsilon}_k/\dot{\epsilon}_b$ is so small for nozzles of larger diameters and at low gas flow rates that it would not really matter whether x is taken as 0 or 1—even with $x = 1$ contribution of $\dot{\epsilon}_k$ to $\dot{\epsilon}$ will be negligible. However, with smaller nozzle diameter and larger gas flow rate, even a small value of x would mean appreciable kinetic energy contribution to the mixing process.

D. *Variation of t_{mix} with Bath Height*

As shown in Figure 6, mixing time decreases with increasing bath height. Similar observations have also been reported by Asai *et al.*[25] and Haida and Brimacombe.[26] Asai *et al.* explained their observations in terms of increase of liquid recirculatory loop length in the vessel with increasing H. Longer circulatory loops result in larger liquid velocity in the bath which, in turn, decreases t_{mix}. Empirical correlation for t_{mix} as a function of various variables obtained by Sano and Mori[30] also supports the view that t_{mix} should decrease with increasing bath height.

In a separate investigation by the authors[41] it has been shown that the plume cone angle is proportional to $H^{-0.374}$. The volume of the plume per unit bath volume (V_P/V_L) is related to plume cone angle (θ_c) in the following manner:

$$\frac{V_P}{V_L} = \frac{1}{6D^2H\tan\left(\frac{\theta_c}{2}\right)}\left[\left(2h\tan\left(\frac{\theta_c}{2}\right) + d_n\right)^3 - d_n^3\right] \quad [5]$$

where D is bath diameter and h is given as (details are given elsewhere[42])

$$h = H + \frac{u_{LP}^2}{2g} \quad [6]$$

Table III. Variation of $\dot{\varepsilon}_k/\dot{\varepsilon}_b$ with Gas Flow Rate, Bath Height, and Nozzle Diameter

		$\dot{\varepsilon}_k/\dot{\varepsilon}_b$													
	$\dot{Q} \times 10^4$ (Nm³/s) = 1.50			8.33			16.67			25.0			33.33		
d_n (mm)	H = 0.10 (m)	0.30	0.45	0.10	0.30	0.45	0.10	0.30	0.45	0.10	0.30	0.45	0.10	0.30	0.45
2.77	0.41	0.122	0.093	12.7	3.8	2.7	50.7	15.2	11.1	114.0	38.4	25.8	202.6	68.2	45.8
3.87	0.108	0.031	0.024	3.3	1.0	0.8	13.3	4.0	2.9	29.9	10.1	6.7	53.2	17.0	12.0
6.66	0.012	0.0036	0.0028	0.38	0.11	0.09	1.52	0.45	0.33	3.4	1.15	0.77	6.1	2.0	1.37
10.0	0.0024	0.0007	0.0005	0.075	0.02	0.017	0.30	0.09	0.07	0.67	0.23	0.15	1.19	0.40	0.27

Table IV. Operating Variables and Their Ranges Employed for Mixing Time Measurements with the Long Columnar Vessel of 0.125 m Diameter and 1.10 m Height

Variable	Range
Gas flow rate, $\dot{Q} \times 10^4$ (Nm³/s)	0 to 1.50
Bath height, H (m)	0.10, 0.15, 0.20, 0.25, 0.30, 0.35, 0.40, 0.45, 0.50, 0.60
Nozzle diameter, d_n (mm)	1.60

where u_{LP} is average liquid velocity inside the plume and is obtained through quantitative analysis of the mixing process.[42] Calculations performed on the basis of this information show that the ratio V_P/V_L increases with increasing H (Figure 17) and that the increase is more rapid at higher gas flow rates. Larger value of V_P/V_L will enhance the liquid circulation flow rate which is also predicted by a mathematical model developed by the authors.[42] Enhanced liquid recirculatory flow rates in the vessel cause faster circulation of the liquid to and from the plume which results in reduced mixing time. Sahai and Guthrie[43] also observed enhanced liquid circulation speeds with increased bath height.

Extrapolation of this experimental observation, however, tends to suggest that the mixing would be instantaneous for a bath of infinite height. This is not physically possible. It is, therefore, logical to expect that t_{mix} would decrease with increasing H up to a certain height only beyond which it would start increasing again. As it was not possible to verify experimentally this speculation using the main experimental set-up because of its limited height, a long glass column of 0.125 mm diameter and 1.10 m length replaced the plexiglass vessel in the main experimental set-up. Various operating variables and their ranges which were examined in these sets of experiments are given in Table IV.

Variation of t_{mix} with H at two different gas flow rates is shown in Figure 18. Because of the scatter in the data, no attempt was made to draw distinct curves for the two flow rates. However, it is evident that t_{mix} decreased with increasing H up to a certain height after which it started increasing. Visual observations of the plume in these experiments also revealed that the plume structure itself changed with increased H. The swirling motion of the plume virtually converted the bath into a bubble column (liquid bath with completely dispersed gas bubbles). This was more pronounced at increased $\dot{Q}$ and H.

As the bath height increases, the hydrodynamic conditions in the bath change. There have been many studies with bubble dispersed liquid baths,[44,45,46] with H/D ratio as high as 10. In the 'multiple circulation model' it has been assumed that the bath consists of several circulation cells in the axial direction, as shown in Figure 19. It is expected that the liquid flow pattern in a bubble column will be quite different from that in a bath with single circulatory loop. Since in the bath of 0.50 m height the ratio H/D in the columnar vessel of the present study is about 4, the bubble column which was observed during the experiments may be treated as the one consisting of multiple circulation cells. In general, mixing results from a combination of many phenomena, *viz.*, molecular diffusion, convective (or bulk) flow, and turbulent (or eddy) diffusion.[29,47] It has already been pointed out that only macromixing (by bulk flow and eddy diffusion) has been studied in the present investigation. In the large vessel, both bulk flow and eddy diffusion are effective. However, in the bubble column there are mul-

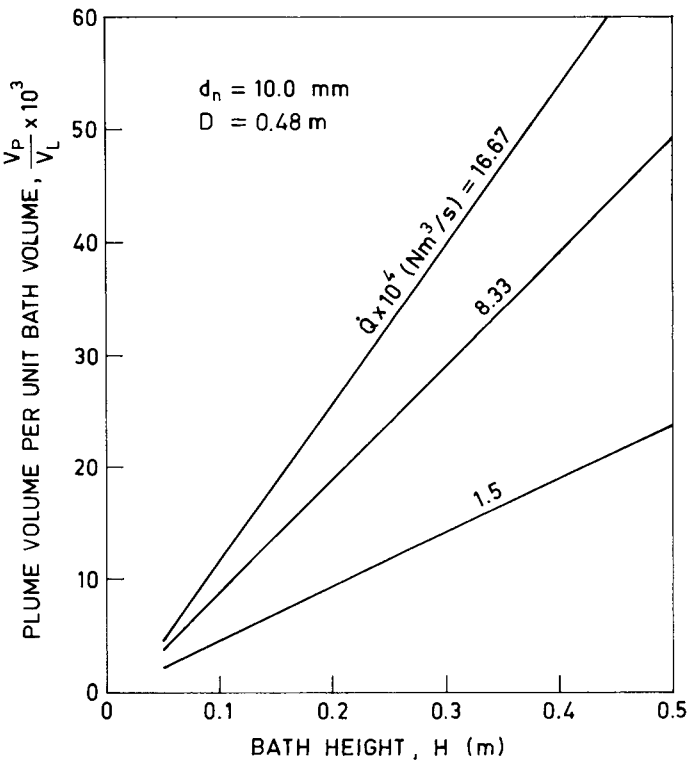

Fig. 17—Variation of plume volume per unit bath volume with bath height for a nozzle of 10.0 mm diameter.

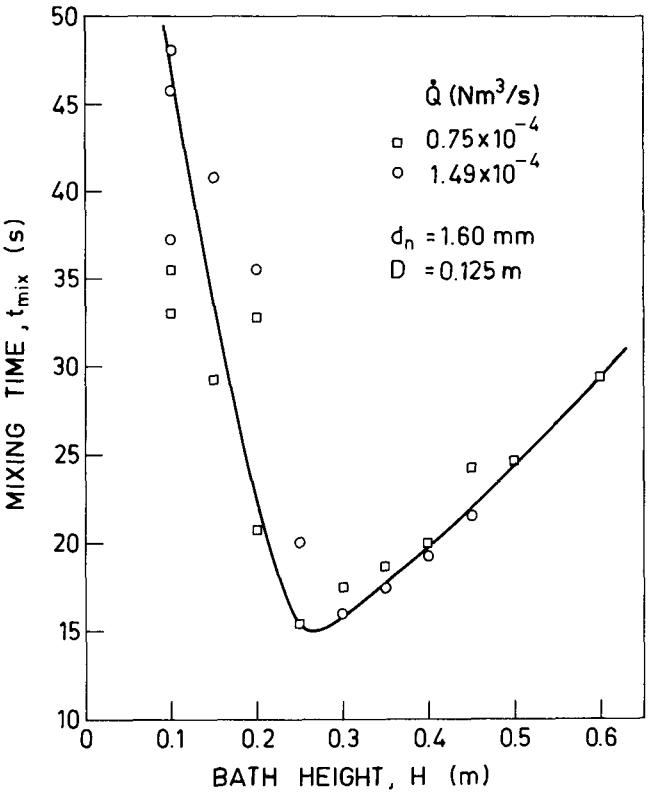

Fig. 18—Variation of mixing time with bath height at two different gas flow rates for the experiments in the vessel of 0.125 m diameter and 1.10 m length.

tiple circulation loops which make mixing by bulk flow ineffective. This is recognized as one of the main causes of increase of t_{mix} with increasing H in a bubble column.

V. MIXING TIME AS FUNCTION OF $\dot{\varepsilon}$

As mentioned above, t_{mix} can be expressed as a function of $\dot{\varepsilon}$, provided the value of the fraction of gas kinetic energy contribution to mixing, x, is known. The value of x could be estimated for various operating conditions using the approach outlined in one of the earlier sections. With these values of x, $\dot{\varepsilon}$ was calculated and the plots of ln t_{mix} *vs* ln $\dot{\varepsilon}$ obtained. One such plot is shown in Figure 20. Then the data, on a logarithmic plot, were least square fitted into two separate interconnected straight lines for two different regimes of gas flow rates. In the lower range of gas flow rate at which swirling motion of the plume is absent, t_{mix} is given as

$$t_{mix} = c_1 \dot{\varepsilon}^{-n_1} \quad [7]$$

whereas at higher gas flow rates which cause the plume to swirl, t_{mix} is expressed as

$$t_{mix} = c_2 \dot{\varepsilon}^{-n_2} \quad [8]$$

c_1, c_2 and n_1, n_2, which are empirical parameters, could be estimated using regression analysis. The values of these parameters for eight different bath heights are presented in Table V.

The estimated n_2 values fall within the range 0.23 to 0.45 as reported by various other investigators,[17,25] who assumed one single equation of the form $t_{mix} = c\dot{\varepsilon}^{-n}$ for the entire range of gas flow rates. n_1 values in our case are, however, lower than these n values. Asai *et al.*[25] are the only other investigators who reported two different equations for different ranges of gas flow rates, but they found n_1 and n_2 to be independent of H. However, in the present study, they are clearly functions of H (Table V) such that n_1 increases and n_2 decreases with increasing H. Since both the mixing rates and the onset of swirling of the plume are dependent on the bath height, the variation of n_1 and n_2 with H is, in fact, expected.

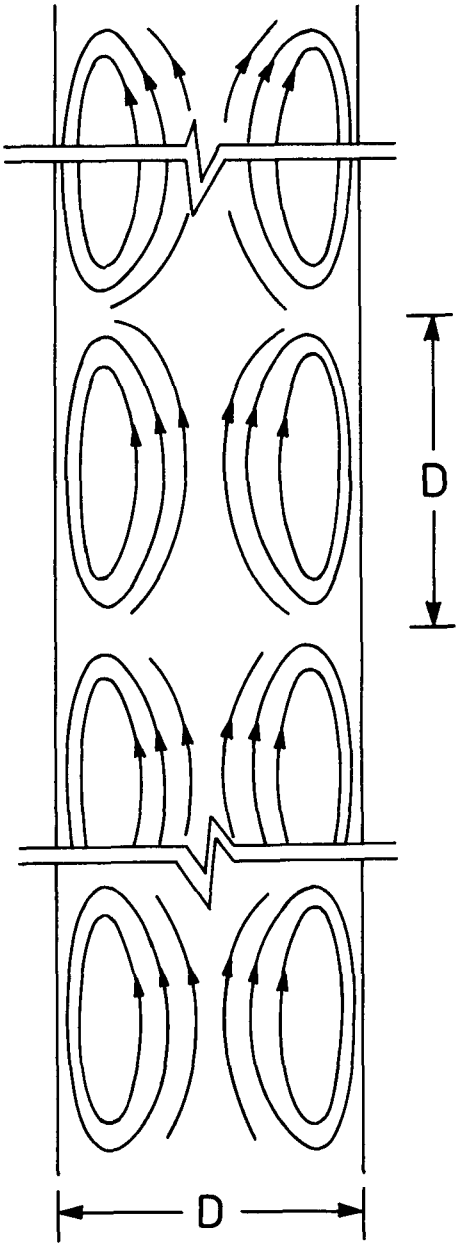

Fig. 19—Schematic representation of multiple circulation loops in a bubble column.[46]

VI. CONCLUSIONS

Mixing in a room temperature water bath, stirred with air blown from the bottom of vessel through a straight circular

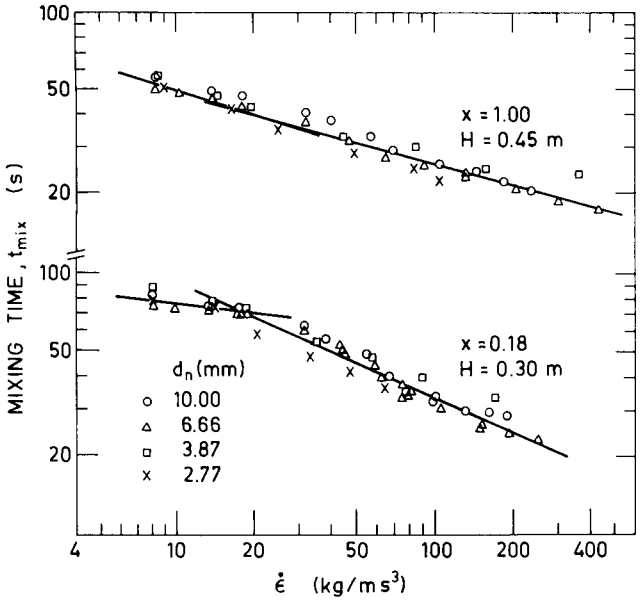

Fig. 20—Variation of mixing time with $\dot{\epsilon}(\dot{\epsilon}_b + x\dot{\epsilon}_k)$ for two different bath heights after incorporating the right value of x.

nozzle fitted axially, was characterized by experimentally determining mixing time (t_{mix}) using an electrical conductivity probe. Bath diameter (D) was 0.48 m for all investigations except for the ones with large H/D ratio where it was 0.125 m. t_{mix} was defined at 0.995 degree of mixing. Measurements were repeated several times to check the reproducibility of the results. Measurements were made employing three probes of different sizes, several probe locations and tracer injection points, and varying amounts of tracer. It was observed that t_{mix} did not depend on these variables. t_{mix} was measured at different gas flow rates, bath heights, and with four nozzles of different sizes. From these experimental investigations the following conclusions were drawn:

1. t_{mix} decreased with increasing gas flow rate and bath height, but decreasing nozzle diameter. Decrease in t_{mix} with decreasing d_n was not significant with nozzles of larger diameter but it was substantial with nozzles of smaller sizes.
2. Plots of ln t_{mix} *vs* ln $\dot{\epsilon}_b$ showed a transition. It was correlated with the onset of swirling of the plume which enhanced the mixing rates in the bath.
3. Experimental data were analyzed to determine the fraction of $\dot{\epsilon}_k$ contributed to mixing. Total mixing energy per unit bath volume ($\dot{\epsilon}$) was defined as $\dot{\epsilon} = \dot{\epsilon}_b + x\dot{\epsilon}_k$. The analysis revealed that x is a function of bath height being negligible at smaller bath heights and almost 1 at larger bath heights.
4. Decrease in t_{mix} with increasing bath height was observed only up to a certain value beyond which it started increasing. Visual examination of the bath revealed that the bath becomes bubble column at large bath heights, thus leading to increase in t_{mix} with increasing bath height.
5. Experimental data, for a particular bath height, were fitted into two separate straight lines in two different regimes of gas flow rates of the form

$$t_{mix} = c_1 \dot{\epsilon}^{-n_1}$$

Table V. Values of c_1, c_2, n_1, and n_2 for Different Bath Heights for Bath Diameter of 0.48 m

H (m)	n_1	n_2	c_1	c_2
0.10	0.138	0.438	180.9	441.5
0.15	0.147	0.492	170.0	472.6
0.20	0.044	0.508	90.9	446.7
0.25	0.139	0.464	122.2	327.1
0.30	0.116	0.442	98.9	258.5
0.35	0.183	0.357	102.3	165.3
0.40	0.257	0.292	102.3	112.8
0.45	0.307	0.280	101.0	95.8

and

$$t_{mix} = c_2 \dot{\epsilon}^{-n_2}$$

n_1 increased and n_2 decreased with increasing bath height, whereas c_1 and c_2 decreased with increasing bath height.

LIST OF SYMBOLS

a	empirical constant defined by Eq. [3]
c_1, c_2	empirical constants defined by Eqs. [7] and [8], respectively
D	bath diameter (m)
d_n	nozzle diameter (mm)
g	acceleration due to gravity (m/s^2)
H	bath height (m)
h	defined by Eq. [6] (m)
n, n_1, n_2	empirical constants defined by Eqs. [3], [7], and [8], respectively
P_{atm}	atmospheric pressure (N/m^2)
Q	gas flow rate (Nm^3/s)
s	standard error (dimensionless)
T_L	liquid temperature (K)
t_{mix}	mixing time (s)
u_{LP}	average liquid velocity inside plume (m/s)
V_L	bath volume (m^3)
V_P	plume volume (m^3)
x	fraction of gas kinetic energy contribution to mixing (dimensionless)
Y	degree of mixing (dimensionless)
$\dot{\epsilon}$	rate of energy dissipation per unit bath volume (kg/ms^3)
$\dot{\epsilon}_b$	rate of buoyancy energy per unit bath volume (kg/ms^3)
$\dot{\epsilon}_{bc}$	it corresponds to transition in ln t_{mix} *vs* ln $\dot{\epsilon}_b$ plots (kg/ms^3)
$\dot{\epsilon}_{bs}$	it corresponds to onset of swirling motion of plume (kg/ms^3)
$\dot{\epsilon}_k$	rate of gas kinetic energy per unit bath volume (kg/ms^3)
θ_c	plume cone angle (deg)
ρ_G	gas density (kg/m^3)
ρ_L	liquid density (kg/m^3)

REFERENCES

1. B. Öhman and T. Lehner: *SCANINJECT I, Proc. of Int. Conf. on Injection Metallurgy*, Jernkontoret, Sweden, 1977.
2. H.-P. Hastert and H. Richter: *Proc. Int. Symp. on Modern Developments in Steelmaking*, Jamshedpur, India, 1981, pp. 75-83.

3. R. Baker, A. S. Normanton, G. D. Spenceley, and R. Atkinson: *Ironmaking and Steelmaking*, 1980, vol. 7, pp. 227-38.
4. R. Henrion: *Ironmaking and Steelmaking*, 1980, vol. 7, pp. 239-41.
5. M. Saigusa, J. Nagai, F. Sudo, H. Bada, and S. Yamada: *Ironmaking and Steelmaking*, 1980, vol. 7, pp. 242-48.
6. N. El-Kaddah and J. Szekely: *SCANINJECT III, Proc. of Int. Conf. on Injection Metallurgy*, Jernkontoret, Sweden, 1983.
7. P. V. Danckwarts: *Chem. Engg. Sci.*, 1958, vol. 8, pp. 93-102.
8. R. W. MacDonald and L. P. Edger: *Chem. Engg. Prog.*, 1951, vol. 47, pp. 363-69.
9. J. B. Gray: *Chem. Engg. Prog.*, 1963, vol. 59, pp. 55-59.
10. C. J. Hoogendoorn and A. P. Denttartog: *Chem. Engg. Sci.*, 1967, vol. 22, pp. 1689-99.
11. C. K. Coyle, H. E. Hirschland, B. J. Michel, and J. Y. Oldshue: *AIChE Journal*, 1970, vol. 16, pp. 903-06.
12. F. Oeters, H. C. Dromer, and J. Kepura: *SCANINJECT III, Proc. of Int. Conf. on Injection Metallurgy*, Jernkontoret, Sweden, 1983.
13. S. C. Koria and K. W. Lange: *Arch. Eisenhüttenwes.*, 1984, vol. 55, pp. 97-100.
14. H. C. Dromer, J. Mietz, F. Oeters, and S. Scheider: *Proc. of Shenyang Symposium on Injection Metallurgy and Secondary Refining of Steel*, Ministry of Metallurgical Industry, China, 1984.
15. V. W. Mohle and B. Vuesser: *Chem. Ing. Tech.*, 1952, vol. 24, p. 494.
16. J. Y. Oldshue, H. E. Hirschland, and A. T. Gretton: *Chem. Engg. Prog.*, 1956, vol. 52, pp. 481-84.
17. K. Nakanishi, T. Fujii, and J. Szekely: *Ironmaking and Steelmaking*, 1975, vol. 2, pp. 193-97.
18. U. P. Sinha and M. J. McNallan: *Metall. Trans. B*, 1985, vol. 16B, pp. 850-53.
19. J. G. Vande Vusse: *Chem. Engg. Sci.*, 1955, vol. 4, pp. 178-200.
20. H. Kramers, G. M. Baars, and W. H. Knoll: *Chem. Engg. Sci.*, 1953, vol. 2, pp. 35-42.
21. D. E. Lamb, F. S. Manning, and R. H. Wilhelm: *AIChE Journal*, 1960, vol. 6, pp. 682-85.
22. L. H. Lehrer: *I and EC Proc. Des. Dev.*, 1968, vol. 7, pp. 226-39.
23. V. Navak and F. Rieger: *Trans. I Chem. E*, 1969, vol. 47, p. T335.
24. A. G. C. Lane and P. Rice: *Trans. I Chem. E*, 1982, vol. 60, pp. 171-76.
25. S. Asai, T. Okamoto, and Ji-Cheng He: *Trans. ISIJ*, 1983, vol. 23, pp. 43-50.
26. O. Haida and J. K. Brimacombe: *SCANINJECT III, Proc. of Int. Conf. on Injection Metallurgy*, Jernkontoret, Sweden, 1983.
27. D. Oymo and R. I. L. Guthrie: *Proc. of 4th Process Technology Conference*, TMS-AIME (ISS), 1984.
28. D. E. Ford, R. A. Mashelkar, and J. Ulbrect: *Proc. Tech. Inst.*, 1982, vol. 17, p. 803.
29. R. I. L. Guthrie: *Iron and Steelmaker*, 1982, vol. 9, pp. 41-45.
30. M. Sano and K. Mori: *Trans. ISIJ*, 1983, vol. 23, pp. 169-75.
31. W. Yoshio, Ji-Cheng He, S. Asai, and I. Muchi: *Tetsu-to-Hagané*, 1983, vol. 69, pp. 1160-66.
32. N. B. Ballal and A. Ghosh: *Metall. Trans. B*, 1981, vol. 12B, pp. 525-34.
33. N. B. Ballal: Ph.D. Thesis, Indian Institute of Technology, Kanpur, India, 1980.
34. S. Nagata: *Mixing Principles and Applications*, John Wiley and Sons, New York, NY, 1975, pp. 171-214.
35. G. G. Krishna Murthy: Ph.D. Thesis, Indian Institute of Technology, Kanpur, India, 1986.
36. G. G. Krishna Murthy, S. P. Mehrotra, and A. Ghosh: *Proc. of 5th Process Technology Conference*, TMS-AIME (ISS), 1986.
37. R. S. Broadkey: *Turbulence in Mixing Operations—Theory and Applications to Mixing and Reaction*, Academic Press, New York, NY, 1975, pp. 47-119.
38. S. M. Bhavaraju, T. W. F. Russell, and H. W. Blanch: *AIChE Journal*, 1978, vol. 24, pp. 454-66.
39. T. C. Hsiao, T. Lehner, and B. Kjellberg: *Scand. J. Metallurgy*, 1980, vol. 9, pp. 105-10.
40. N. J. Themelis and P. Goyal: *Can. Met. Quart.*, 1983, vol. 22, pp. 313-20.
41. G. G. Krishna Murthy, A. Ghosh, and S. P. Mehrotra: *Metall. Trans. B*, 1988, vol. 19B, pp. 885–92.
42. G. G. Krishna Murthy, A. Ghosh, and S. P. Mehrotra: *Metall. Trans. B*, in press.
43. Y. Sahai and R. I. L. Guthrie: *Metall. Trans. B*, 1982, vol. 13B, pp. 193-202.
44. P. B. Whalley and J. F. Davidson: *Proc. of Symposium on Multiphase Flow Systems* (Symp. S. No. 38), Instn. Chem. Engr., London, 1974.
45. J. B. Joshi and M. M. Sharma: *Trans. I Chem. E*, 1976, vol. 54, p. 42.
46. J. B. Joshi and M. M. Sharma: *Trans. I Chem. E*, 1979, vol. 57, pp. 244-51.
47. V. W. Uhl and J. B. Gray: *Mixing—Theory and Practice*, Academic Press, New York, NY, 1966, vol. I, pp. 7-110.